Infrared spectroscopic and computational studies on formamide solutions of Ca^<2+>. Vibrational frequencies of formamide and modes of coordination to Ca^<2+>

Ohashi, Kazuhiko
Department of Chemistry, Faculty of Science, Kyushu University

Hikiishi, Nobutaka
Department of Chemistry, Graduate School of Science, Kyushu University

Takeshita, Hayato
Department of Chemistry, Graduate School of Science, Kyushu University

出版情報：Spectrochimica Acta Part A: Molecular and Biomolecular Spectroscopy. 206, pp.112-119, 2019-01-05. Elsevier
バージョン：
権利関係：

Infrared spectroscopic and computational studies on formamide solutions of Ca^{2+}. Vibrational frequencies of formamide and modes of coordination to Ca^{2+}

Kazuhiko Ohashi [a,*], Nobutaka Hikiishi [b], Hayato Takeshita [b]

[a] *Department of Chemistry, Faculty of Science, Kyushu University, Motooka, Fukuoka 819-0395, Japan*

[b] *Department of Chemistry, Graduate School of Science, Kyushu University, Motooka, Fukuoka 819-0395, Japan*

ABSTRACT

Infrared spectroscopy for formamide (FA) solutions of $Ca(ClO_4)_2$ shows that both CN stretch (ν_{CN}) and CO stretch (ν_{CO}) bands of FA undergo upshifts in the presence of Ca^{2+}. Modeling of Ca^{2+} in FA solutions is accomplished by quantum chemical calculations for $Ca^{2+}(FA)_n$ (n = 1–8) complexes with Polarizable Continuum Model (PCM). The calculations indicate that bidentate $Ca^{2+}(FA)_4$ complexes are not consistent with the observed upshift of the ν_{CN} band, although a bidentate coordination of four FA molecules via both O and N atoms was assumed in a previous study of the same system. The experimental results are reasonably reproduced by adopting $Ca^{2+}(FA)_7$ and $Ca^{2+}(FA)_8$ complexes with a monodentate coordination of all FA molecules via the O atom. A strong coupling among the CO oscillators is shown to be responsible for the upshifts of the ν_{CO} modes despite the O atom coordination.

Keywords:

Formamide; Calcium (II) ion; Infrared spectroscopy; Quantum chemical calculations; Coordination modes; Intermolecular interactions

---

* Corresponding author.

E-mail address: kazu@chem.kyushu-univ.jp (K. Ohashi).

1. Introduction

Interactions of metal ions and biologically relevant ligands have attracted much interest from a variety of points of view [1,2]. In particular, amide and urea molecules contain both oxygen and nitrogen atoms as binding sites for metal cations. Metal complexes of amides and ureas show coordination through the O atom almost exclusively [3], because the O atom is usually more basic than the N atom. Nevertheless, exceptional complexes were reported in which Ni^{2+} and Cu^{2+} bind to the N atom of substituted ureas [3].

Formamide (FA) is the simplest molecule containing a peptide group. FA is not well represented by the single Lewis structure I and its planar geometry needs to be understood in terms of strong resonance mixing of the ionic structure II.

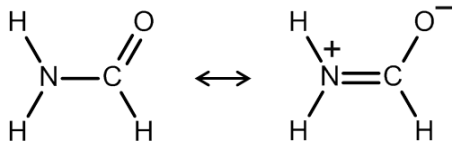

I II

In structure I, the CN bond has a single-bond character while the CO bond has a double-bond character, but the two bonds interchange characters in structure II. Accordingly, the contribution of each structure to the resonance hybrid is best probed through vibrational spectroscopy. Rao and coworker observed a lowering of the CO stretch (ν_{CO}) frequency by infrared (IR) spectroscopy of lithium salts dissolved in various amides and suggested that the Li^+ ion binds to the O atom of amides [4]. Meanwhile, Rode carried out ab initio calculations of the $Li^+(FA)_2$ complexes in a chelate configuration [5]. Through Raman spectroscopy of alkali and alkaline-earth metal salts dissolved in FA, Lees et al. proposed that structure II becomes major under the effects of dissolved electrolytes and that the metal ion binds to the O atom of FA [6,7]. This proposal was based on the idea that structure II should be favorable for the coordination via the O atom, because the O atom is more negative in II than in I. Powell and Woollins recorded IR and Raman spectra for complexes of FA with a series of transition metals and pointed out that the downshifts of the ν_{CO} and δ_{NCO} bands in combination with the upshift of the ν_{CN} band should be viewed as evidence for the O atom

coordination [8]. Bukowska studied FA solutions of Li^+, Na^+, and Ca^{2+} by Raman and IR spectroscopy [9,10]. An upshifted component was newly observed in the ν_{CO} region when the salts were dissolved in FA [10], in striking contrast to the downshift reported in the previous studies [4,6–8]. More recently, Alves and coworkers reported vibrational spectroscopic studies on FA molecules interacting with a metal ion of various types. Upshifts of both ν_{CO} and ν_{CN} bands were observed in the presence of Li^+ [11], Ca^{2+} [12], and Al^{3+} [13]. Since the upshift of the ν_{CO} band was inconsistent with the O atom coordination, Alves and coworkers assumed a bidentate coordination through both O and N atoms in a chelate configuration. However, it is not obvious whether the bidentate coordination is consistent with the upshifts of both ν_{CO} and ν_{CN} modes or not.

In the present work, we have carried out IR spectroscopic studies of FA solutions of $Ca(ClO_4)_2$. We have also performed theoretical calculations for optimizing geometries and predicting vibrational spectra of $Ca^{2+}(FA)_n$ (n = 4–8) complexes as a model of Ca^{2+} in FA solutions. We aim at revealing the effect of $Ca^{2+}\cdots$FA and FA$\cdots$FA interactions on the intramolecular vibrations of FA, in particular the ν_{CO} and ν_{CN} modes. We have found that the generally accepted idea about the frequency shifts of FA upon coordination is not entirely true.

2. Experimental and computational methods

IR spectra are recorded on a Fourier transform IR spectrometer (JASCO, FT/IR-4100) using an attenuated total reflection (ATR) unit (ATR PRO670H-S) with a ZnSe prism. ATR-IR spectra are obtained in the 650–4000 cm^{-1} region with a resolution of 2 cm^{-1}. $Ca(ClO_4)_2$ is used as a source of Ca^{2+}, because it is expected that the ClO_4^- anion hardly distorts the first coordination sphere of Ca^{2+} owing to a smaller charge density on ClO_4^- than on Cl^- [12]. Calcium perchlorate (Strem) and FA (Wako) are used as received. The salt is added to FA to prepare solutions with concentrations in the range of 1.0–4.0 M.

Theoretical calculations are carried out with GAUSSIAN 16 program package [14] by using computer facilities (Fujitsu, PRIMERY CX2550/CX2560 M4) at Research Institute for

Information Technology in Kyushu University. We employ the density functional theory (DFT) method using the Becke's three parameter hybrid functional coupled with the Lee–Yang–Parr correlation functional (B3LYP) and the second-order Møller–Plesset perturbation (MP2) method for selected species. Basis sets used are 6-311+G(2df) for Ca and 6-31+G(d) for other atoms. Self-consistent reaction field method with Polarizable Continuum Model (PCM) is incorporated to implicitly account for extra solvent molecules surrounding the species of interest. Geometries of $Ca^{2+}(FA)_n$ (n = 1–8) complexes and other species in PCM are optimized without any symmetry constraints; it is confirmed that the resulting structures have no imaginary-frequency vibration unless otherwise stated. It is generally accepted that vibrational frequencies of gas-phase clusters are better predicted by DFT than MP2 calculations [15]. Experimental values for vibrational frequencies of FA molecule in the gas phase are available in the literature [16]. Harmonic frequencies of FA in vacuum are calculated at the B3LYP/6-31+G(d) level and scaling factors are evaluated for each fundamental vibration. The results are 0.978 for the CH scission and 0.973 for an average of nine fundamental vibrations above 1000 cm^{-1}. Harmonic frequencies of all vibrations, except the CH scission, of all species in PCM are scaled with the average factor of 0.973 and the CH scission frequencies are scaled with its own factor of 0.978. The scaled frequencies and IR as well as Raman intensities are displayed as stick diagrams in the figures of this article.

3. Results and discussion

3.1. IR spectra of FA and FA solutions of $Ca(ClO_4)_2$

Fig. 1a shows an ATR-IR spectrum of neat FA liquid in the 1200–1800 cm^{-1} region. The spectrum exhibits four bands with maxima around 1307, 1390, 1610, and 1673 cm^{-1}, which are assigned to the CN stretch (ν_{CN}), CH scission (δ_{CH}), HNH scission (δ_{HNH}), and CO stretch (ν_{CO}) bands, respectively [16,17]. Fig. 1b–e demonstrates changes in the spectra accompanied by gradual addition of $Ca(ClO_4)_2$. With increasing the concentration, both ν_{CN} and ν_{CO} bands undergo gradual upshifts, the δ_{HNH} band undergoes a gradual downshift, and the δ_{CH} band remains almost unshifted. In the spectrum of 4.0 M solution, the ν_{CN}, δ_{CH},

δ_{HNH}, and ν_{CO} bands show maxima around 1321, 1393, 1595, and 1683 cm^{-1}, respectively. These spectral changes are in agreement with those observed in Raman spectroscopy carried out by Silva and Alves [12]. As pointed out by these authors, the upshifts of both ν_{CN} and ν_{CO} bands are not explainable with a change in the contribution of Lewis structures I and II.

3.2. Metal–ligand interactions in $Ca^{2+}(FA)_1$

Theoretical calculations are performed to predict the direction and magnitude of the shifts of the ν_{CN} and ν_{CO} modes when the metal ion interacts with either of the O atom, the N atom, or both of FA molecule. Fig. 2 displays the optimized structures and theoretical IR spectra for FA monomer and four isomers of $Ca^{2+}(FA)_1$ complexes from DFT calculations. Two isomers are found for the O-bound geometry, where Ca^{2+} is bound to the O atom of FA. In one isomer 1-O-i, Ca^{2+} and NH_2 group are on the opposite sides of the CO bond; this configuration is referred to as 'trans' in this article. In the other isomer 1-O-ii, Ca^{2+} and NH_2 group are on the same side; this configuration is referred to as 'cis'. In an N-bound isomer 1-N, Ca^{2+} is bound to the N atom with the Ca···N distance of 2.83 Å. In a bidentate isomer 1-ON, Ca^{2+} is bound to both O and N atoms with the Ca···O and Ca···N distances of 2.74 and 2.56 Å, respectively. In order to achieve the bidentate coordination, the HCO group is internally rotated by ≈50° about the C–N axis from the original molecular plane. Although FA molecules remain planar in the O-bound isomers, the N atom of 1-N and 1-ON undergoes pyramidalization, which is characteristic of Lewis structure I. Therefore, the pyramidalization can be regarded as an indication of the interaction between the N atom and the metal ion. Table S1 of Supplementary material (SM) collects charges on Ca, O, C, and N atoms for selected species. On going from FA to 1-O-i and 1-O-ii, the O atom becomes more negative while the N atom becomes less negative. On going from FA to 1-N, on the other hand, the O atom becomes less negative while the N atom becomes more negative. MP2 calculations are carried out for re-optimizing the geometry and estimating the relative energy of four isomers. Although the structures by MP2 calculations are slightly different from those by DFT calculations, the same labels are used to identify the isomers. 1-O-i is

lowest in energy and 1-O-ii is higher by 2 kJ mol^{-1}. 1-N and 1-ON lie 39 and 42 kJ mol^{-1} above 1-O-i, respectively.

In the theoretical IR spectra from DFT calculations, the ν_{CN} and ν_{CO} transitions of the FA monomer in PCM are located at 1266 and 1681 cm^{-1}, respectively. The ν_{CN} and ν_{CO} transitions of 1-O-i are located at 1321 and 1665 cm^{-1}, respectively, resulting in an upshift (+55 cm^{-1}) of ν_{CN} and a downshift (–16 cm^{-1}) of ν_{CO}. The same transitions of 1-O-ii are located at 1318 and 1669 cm^{-1}, resulting in an upshift (+52 cm^{-1}) of ν_{CN} and a downshift (–12 cm^{-1}) of ν_{CO}. The direction of these shifts is consistent with an increased contribution of Lewis structure II, as is supported by changes in the atomic charges (Table S1 of SM). On the other hand, the ν_{CN} and ν_{CO} transitions of 1-N are located at 1226 and 1722 cm^{-1}, respectively, resulting in a downshift (–40 cm^{-1}) of ν_{CN} and an upshift (+41 cm^{-1}) of ν_{CO}. The direction of these shifts is consistent with an increased contribution of Lewis structure I. In this manner, we can confirm an intuitive idea about the shifts of ν_{CN} and ν_{CO} upon complexation with the metal ion. For the bidentate complex 1-ON, however, the direction of the shifts of ν_{CN} and ν_{CO} is not obvious. DFT calculations locate the ν_{CN} and ν_{CO} transitions at 996 and 1644 cm^{-1}, respectively, resulting in a downshift (–270 cm^{-1}) of ν_{CN} and a downshift (–37 cm^{-1}) of ν_{CO}. The downshifts of both ν_{CN} and ν_{CO} bands cannot be explained by a change in the contribution of Lewis structures I and II, although Silva and Alves proposed a stabilization of structure I through a bidentate coordination [12]. The point is that the ν_{CN} mode undergoes a downshift when FA is bound to Ca^{2+} via the N atom, irrespective of whether the coordination is monodentate or bidentate.

3.3. Ligand–ligand interactions in $Ca^{2+}(FA)_2$

Theoretical calculations are continued to examine the effect of ligand–ligand interactions on the vibrations of FA. Fig. 3 illustrates the structures and theoretical IR spectra for four isomers of $Ca^{2+}(FA)_2$ complexes from DFT calculations. Isomers 2-O-i, 2-O-ii, and 2-ON* are formed by adding a second FA molecule opposite the first one in 1-O-i, 1-O-ii, and 1-ON, respectively, with a coordination configuration similar to the first one. Both 2-O-i

and 2-O-ii are stationary structures located at potential-energy minima. On the other hand, 2-ON* is not a stationary but an instantaneous geometry during an optimization process. In this article, an asterisk symbol attached to the structure label indicates that it is a non-stationary structure. All attempts fail to find a potential-energy minimum corresponding to 2-ON*; the optimization processes end up with structures in which two FA molecules adopt monodentate coordinations. In another instantaneous geometry 2-O-iii*, the Ca^{2+} ion is squeezed into the center of a ring dimer of $(FA)_2$ (cf. section 3.6). A similar structure was proposed for $Li^+(FA)_2$ and referred to as 'chelate' complex [5,10]. It was claimed that two NH···O hydrogen bonds in the ring dimer were remaining and Li^+ was interacting with both O and N atoms of FA in the 'chelate' complex [5]. Then attempts are made to find a potential-energy minimum corresponding to such a 'chelate' complex, but the geometry optimizations always converge to monodentate complexes. In 2-O-iii*, the intermolecular NH···O distances are 3.80 Å, which are too long to be viewed as hydrogen bonds. The Ca^{2+}···N distances (2.83 Å) are longer than the Ca^{2+}···HN distances (2.35 Å). In addition, two FA molecules in 2-O-iii* remain planar, implying that the interaction between the Ca^{2+} ion and the N atom of FA is negligibly small. Accordingly, we classify 2-O-iii as an O-bound geometry. From MP2 calculations, 2-O-i is lowest in energy and 2-O-ii is higher by 4 kJ mol^{-1}. MP2 calculations again fail to find potential-energy minima corresponding to bidentate and 'chelate' complexes. Geometries similar to 2-ON* and 2-O-iii* lie >100 and >200 kJ mol^{-1} above 2-O-i, respectively.

Overall spectral features of 2-O-i and 2-O-ii are similar to those of 1-O-i and 1-O-ii, respectively. The ν_{CN} transition of 2-ON* is downshifted, which is characteristic of the Ca^{2+}···N interaction, as described in section 3.2. In the so-called 'chelate' structure 2-O-iii*, the ν_{CO} transition undergoes a large downshift and switches position with the δ_{HNH} transition. The ν_{CN} transition of 2-O-iii* is also downshifted, although the N atom is not pyramidalized in this geometry.

Two FA molecules are nearly equivalent to each other in all $Ca^{2+}(FA)_2$ isomers. In each isomer, there is a coupling between the CO oscillators in FA molecules. This coupling

gives rise to a splitting of the ν_{CO} modes into two normal modes; two CO oscillators vibrate out-of-phase in one mode and in-phase in the other. The frequencies of the two modes are as follows: 1666/1670 cm^{-1} for 2-O-i, 1665/1670 cm^{-1} for 2-O-ii, 1696/1696 cm^{-1} for 2-ON*, and 1608/1613 cm^{-1} for 2-O-iii. Only the former mode of each isomer is IR active. The width of the splitting, denoted by Δ hereafter, depends on the vibration. In the case of 2-O-i, for instance, the width for ν_{CO} is $\Delta = 4$ cm^{-1}, whereas the widths for ν_{CN}, δ_{CH}, and δ_{HNH} are smaller than 1 cm^{-1}. This means that the coupling of the ν_{CO} modes is much stronger than that of other vibrations.

3.4. Interactions of $Ca^{2+}(FA)_1$ with another Ca^{2+}

In concentrated solutions, there would be a possibility of one FA molecule interacting with multiple Ca^{2+} ions [10]. We carry out DFT calculations for $(Ca^{2+})_2(FA)_1$ complexes in which one Ca^{2+} is bound to the N atom and the other to the O atom of FA; the results are depicted in Fig. S1 of SM. Geometry optimizations find stationary structures, but the $Ca^{2+}\cdots$N distances are too long. Then we look at instantaneous geometries (Fig. S1a and b of SM) during optimization processes. In the theoretical spectra for these geometries (Fig. S1d and e of SM), both ν_{CN} and ν_{CO} transitions are downshifted relative to the FA monomer. Of note is that the ν_{CN} modes are downshifted when one Ca^{2+} is bound to the N atom, even when the other Ca^{2+} is bound to the O atom simultaneously.

3.5. Interactions of $Ca^{2+}(FA)_1$ with counter anions

Silva and Alves suggested that the ClO_4^- anion hardly distorts the first coordination sphere of Ca^{2+} [12]. Owing to a small charge density on ClO_4^-, the FA$\cdots ClO_4^-$ interactions are expected to be much smaller than the $Ca^{2+}\cdots$FA interactions. Nevertheless, we need to examine the effect of ClO_4^- in the second sphere on the vibrations of FA molecule in the first sphere. For this purpose, we choose so-called solvent-separated ion pairs consisting of $Ca^{2+}(FA)_1$ (1-O-i) and one or two ClO_4^- ions; the results are displayed in Fig. S2 of SM. The binding of one or two ClO_4^- ions to the NH_2 group of FA results in a further upshift of the ν_{CN}

transition by 10–20 cm^{-1}. The ν_{CO} transition is also upshifted from $Ca^{2+}(FA)_1$, but the magnitude of the shift is smaller (1–5 cm^{-1}). Ion pairs consisting of 1-O-ii show essentially the same features.

3.6. Structures of liquid FA

The definitive structure of liquid FA has not been established yet; models proposed so far include ring dimer, hydrogen-bonded chain, ring dimer and chain, ring hexamer, and so forth. Bakó et al. summarized the conclusions obtained by various experimental and theoretical methods [18]. In order to discuss the effect of Ca^{2+} on the vibrational frequencies of FA, it is convenient to define a theoretical IR spectrum of neat FA liquid for a comparison with theoretical IR spectra of $Ca^{2+}(FA)_n$ complexes. For this purpose, we consider several model clusters of FA in order to mimic the structure of liquid FA. The optimized structures and their IR spectra are shown in Fig. S3 of SM. Pullman et al. suggested that the dominant unit in the structure of liquid FA is one that contains a cyclic dimer and a linear chain held together by hydrogen bonds [19], which is similar to 4RL (Fig. S3c of SM). Since the theoretical spectrum of 4RL is in best agreement with the experimental spectrum, it is regarded as a mimic of the liquid FA spectrum in the analysis presented below.

3.7. Structures and IR spectra of $Ca^{2+}(FA)_4$

Now we try to find a $Ca^{2+}(FA)_n$ complex which can be regarded as a model of Ca^{2+} in FA solutions. We first examine $Ca^{2+}(FA)_4$ complexes, because Silva and Alves proposed that the average number of FA molecules around Ca^{2+} was 4 from an analysis of Raman spectra [12] (cf. section 3.10). Fig. 4 illustrates the geometries of six isomers of $Ca^{2+}(FA)_4$. Since Silva and Alves assumed a 'chelate' coordination [12], we begin with such 'chelate' complexes. Both 4-O-vii* and 4-O-viii* (Fig. 4a and b) are composed of two sets of FA pairs similar to that in 2-O-iii*. In these isomers, four carbon atoms of FA are arranged to form a square plane. In 4-O-vii*, the OCN backbones of FA labeled 1 and 3 are situated in the plane, while those of FA labeled 2 and 4 are nearly perpendicular to the plane. In

4-O-viii*, the OCN backbones of all FA are nearly perpendicular to the plane. Both 4-O-vii* and 4-O-viii* are not stationary but instantaneous geometries during optimization processes. We make efforts to find potential-energy minima corresponding to these geometries, but the optimization processes always end up with monodentate complexes, where four FA molecules are bound to Ca^{2+} via the O atom. Next we consider genuine bidentate complexes. Both 4-ON-i* and 4-ON-ii* (Fig. 4c and d) are composed of two sets of FA pairs similar to that in 2-ON*. Once again, both of them are not stationary but instantaneous geometries during optimization processes. In 4-N* (Fig. 4e) with a monodentate coordination via the N atom, four N atoms of FA adopt a tetrahedral coordination. This geometry is also non-stationary, having one imaginary-frequency vibration. In contrast to the 'chelate', bidentate, and N-bound geometries noted above, a number of stationary structures are found for O-bound isomers. From DFT calculations, the lowest-energy structure is 4-O-i (Fig. 4f), in which four O atoms of FA adopt a square-planar coordination with 'cis' configuration. Other O-bound isomers are treated in Figs. S4 and S5 of SM.

Fig. 5b–g represents the theoretical IR spectra predicted for six geometries of $Ca^{2+}(FA)_4$. Reproduced in Fig. 5a are the experimental spectrum of neat FA liquid and the theoretical spectrum of 4RL. In the spectra of the 'chelate' geometries 4-O-vii* and 4-O-viii*, both ν_{CN} and ν_{CO} transitions are downshifted from those of 4RL. In the spectra of the bidentate geometries 4-ON-i* and 4-ON-ii*, the ν_{CN} transitions are downshifted from those of 4RL, while the ν_{CO} transitions are mostly upshifted. The IR spectra are predicted also for other 'chelate' and bidentate geometries including less symmetric ones; the ν_{CN} transitions are always downshifted, although the ν_{CO} transitions are either downshifted or upshifted depending on the geometry.

From the experimental observation that both ν_{CN} and ν_{CO} bands are upshifted in the Raman spectra, Silva and Alves assumed a 'chelate' coordination, which was interpreted to be a bidentate coordination concurrently [12]. However, our calculations indicate that the ν_{CN} modes of both 'chelate' and bidentate geometries are downshifted; the direction of the shift is in conflict with the results of the previous Raman and present IR spectroscopy. Similarly,

the ν_{CN} modes are downshifted in the spectrum of the N-bound 4-N*. Thus the 'chelate', bidentate, and N-bound complexes of $Ca^{2+}(FA)_4$ are not appropriate for a model of Ca^{2+} in FA solutions. In the spectrum of the O-bound complex 4-O-i, the ν_{CN} transitions are upshifted while the ν_{CO} transitions remain almost unshifted. Let us look at other O-bound $Ca^{2+}(FA)_4$ complexes (Figs. S4 of SM). Fig. S5 of SM demonstrates that, for all O-bound isomers, the positions of the ν_{CN}, δ_{CH}, and δ_{HNH} transitions are in reasonable agreement with those of the experimental spectrum for the 4.0 M solution (Fig. 1e). However, the strongest one of the ν_{CO} transitions is slightly downshifted from that of 4RL, although 4-O-ii, 4-O-iii, 4-O-v, and 4-O-vi exhibit weak ν_{CO} transitions on higher frequency side.

A survey of various model complexes of $Ca^{2+}(FA)_4$ suggests that the O-bound isomers are most appropriate for reproducing the IR spectra of FA solutions of Ca^{2+}. Only the direction of the shift of ν_{CO} is in conflict with the experimental results.

3.8. Structures and IR spectra of O-bound isomers of $Ca^{2+}(FA)_{5–8}$

As described in section 3.7, monodentate rather than bidentate coordinations of FA to Ca^{2+} are feasible. If this is the case, a solvation number of 4, as suggested by Silva and Alves [12], is too small, because a solvation number of 7 was reported for Ca^{2+} solvated with dimethylformamide (DMF) [20]. Then we examine O-bound isomers of $Ca^{2+}(FA)_n$ complexes with n = 5–8. Fig. 6 displays the optimized geometries of the lowest-energy isomers for each n. 5-O-i (Fig. 6a) is formed by adding a fifth FA molecule over the Ca^{2+} ion in 4-O-i. 6-O-i (Fig. 6b) is formed by adding a sixth FA molecule under Ca^{2+} in 5-O-i. 7-O-i and 8-O-i (Fig. 6c and d) are formed by squeezing two and three FA molecules, respectively, in the upper side of Ca^{2+} in 5-O-i. All FA molecules in all complexes are bound to Ca^{2+} with 'cis' configuration. Other types of O-bound isomers are also examined; geometrical structures and theoretical IR spectra for n = 5–8 are presented in Figs. S6–S9 of SM, respectively. As shown in Table S1 of SM, the O atoms in the O-bound isomers become less negative gradually with increasing n, while the charges on the N and C atoms change only slightly.

Fig. 7b–f represents the theoretical IR spectra predicted for the lowest-energy isomers of $Ca^{2+}(FA)_n$ with n = 4–8. Reproduced in Fig. 7a are the theoretical spectrum of 4RL and the experimental spectrum of neat FA liquid. The strongest ν_{CO} transitions of the n = 4–6 complexes are slightly downshifted from that of 4RL; the direction is inconsistent with the experiment. However, the ν_{CO} frequencies gradually increase with increasing n from 6 to 8. The strongest ν_{CO} transitions of the n = 7 and 8 complexes are slightly upshifted from that of 4RL; the direction is consistent with the experiment. An upshift of 11 cm^{-1} from 4RL to 8-O-i is comparable with the observed upshift (≈10 cm^{-1}) of the band maxima from the neat FA liquid to the 4.0 M solution. Meanwhile, all ν_{CN} transitions for n = 4–8 are upshifted from the averaged one of 4RL (1302 cm^{-1}); the direction is consistent with the experiment. Overall, the theoretical IR spectra for 7-O-i and 8-O-i are in agreement with the experimental spectrum of the 4.0 M solution. The most important finding is that the strongest ν_{CO} transitions of 7-O-i and 8-O-i undergo upshifts, in spite of the monodentate coordination via the O atom.

3.9. IR and Raman spectra of O-bound isomers of $Ca^{2+}(FA)_7$ and $Ca^{2+}(FA)_8$

Responding to the success of 7-O-i and 8-O-i in predicting the upshift of the ν_{CO} band, we concentrate on O-bound isomers of $Ca^{2+}(FA)_7$ and $Ca^{2+}(FA)_8$. As described in section 3.3, there is a coupling between the CO oscillators of FA molecules. Since the strength of the coupling should depend on the distance and mutual orientation of the CO oscillators [21], we examine four distinct isomers for each of $Ca^{2+}(FA)_7$ and $Ca^{2+}(FA)_8$. In order to distinguish these isomers, we pay attention to a local dipole moment of the CO bond, which points from the O atom towards the C atom. Fig. S8 of SM displays the optimized structures and theoretical IR spectra; the upper panel of Fig. S10 of SM exhibits the theoretical Raman spectra for four isomers of $Ca^{2+}(FA)_7$. Fig. S9 of SM displays the optimized structures and theoretical IR spectra; the lower panel of Fig. S10 of SM exhibits the theoretical Raman spectra for four isomers of $Ca^{2+}(FA)_8$. It is easier to understand the differences among the n = 8 isomers, because the structures of the n = 8 complexes are more

symmetric than those of the $n = 7$ complexes. Structural differences among four isomers of $Ca^{2+}(FA)_7$ are analogous to those of $Ca^{2+}(FA)_8$. Figs. S9 and S10 of SM show that the ν_{CN} modes of 8-O-i and 8-O-ii are upshifted from the average one of 4RL. On the other hand, the ν_{CN} modes of 8-O-iii and 8-O-iv are downshifted, in spite of the monodentate coordination via the O atom.

Fig. 8 compares the theoretical IR and Raman spectra of 8-O-i with the respective experimental spectra. Fig. S11 of SM makes the same comparison for 7-O-i. As in the case of the IR spectra, there is an overall agreement between the theoretical and experimental Raman spectra. Let us take a closer look at the ν_{CO} modes. Table S2 of SM gathers the scaled ν_{CO} frequencies, IR intensities, and Raman scattering activities of 7-O-i and 8-O-i. Each of the ν_{CO} modes is not localized on a CO group of a particular FA molecule in the complexes, but is a normal mode vibration delocalized over all FA molecules. The highest-frequency mode of 8-O-i at 1708.8 cm^{-1} involves in-phase motions of the CO groups of all FA molecules. The IR intensity of this mode is almost zero because of the symmetry of the structure. On the other hand, the Raman scattering activity of this in-phase mode is largest. Seven other modes of 8-O-i involve out-of-phase motions of the CO groups. Nearly degenerated modes at 1683.3/1683.4 cm^{-1} have the largest IR intensities, but the Raman activities are almost zero. Nearly degenerated modes at 1667.8/1667.9 cm^{-1} have the second largest Raman activity, but the IR intensities are almost zero. The ν_{CO} region of the IR spectrum of the 4.0 M solution is characterized by a single and rather symmetric band at 1683 cm^{-1}. The strong IR transitions of 8-O-i predicted at 1683.3/1683.4 cm^{-1} probably contribute to the 1683 cm^{-1} band. On the other hand, the ν_{CO} region of the Raman spectra reported by Silva and Alves [12] is characterized by a maximum around 1680 cm^{-1} and an appreciable shoulder at 1719 cm^{-1}. The strong Raman transitions of 8-O-i predicted at 1667.8/1667.9 and 1708.8 cm^{-1} probably contribute to the 1680 cm^{-1} maximum and the 1719 cm^{-1} shoulder, respectively. Thus, 8-O-i is successful in reproducing the differences in the characteristic features between the IR and Raman spectra.

As for the δ_{HNH} region, the intensity of the band is underestimated in the theoretical

IR spectrum, whereas overestimated in the theoretical Raman spectrum. We speculate a reason for this as follows. In each of FA molecules bound to Ca^{2+} in 8-O-i, one of the H atoms of the NH_2 group faces outward and a ClO_4^- ion may attach to it in real solutions. The attachment of the counter ion must affect the intensity as well as the position of the δ_{HNH} band, as Fig. S2 of SM reveals that the IR intensity of the δ_{HNH} transition of $Ca^{2+}(FA)_1$ is enhanced by the attachment of ClO_4^-. However, the counter ion is not included in the calculations presented in sections 3.7–3.9.

At the end of this section, let us consider the direction of the shift of the ν_{CO} band. In the previous Raman and present IR spectra, both ν_{CO} and ν_{CN} bands are upshifted in the presence of Ca^{2+}. The upshift of the ν_{CN} band is expected for the O-bound complexes, from the consideration based on the Lewis structures I and II. However, the upshift of the ν_{CO} band is unexpected for the O-bound complexes. Fig. S12 of SM represents a diagram of vibrational energy levels for selected species, which helps us understand the upshift of the ν_{CO} band. As demonstrated in section 3.2, the ν_{CO} transitions of the O-bound $Ca^{2+}(FA)_1$ complexes are downshifted by –16 and –12 cm^{-1} for 1-O-i and 1-O-ii, respectively. This means that a one-to-one interaction between the Ca^{2+} ion and the O atom of FA leads to the downshift; the direction is consistent with the expectation based on the Lewis structures. As described in section 3.3, there is a coupling between the CO oscillators of the $Ca^{2+}(FA)_2$ complexes. In 2-O-i and 2-O-ii, the coupling gives rise to a splitting of the ν_{CO} modes with a width of Δ = 4 and 5 cm^{-1}, respectively. In 4-O-i, four ν_{CO} modes are predicted at 1665, 1670, 1671, and 1683 cm^{-1}; the magnitude of the splitting is Δ = 18 cm^{-1}. In 8-O-i, as listed in Table S2 of SM, the magnitude of the splitting is Δ = 41 cm^{-1}, which is much larger than the magnitude of the downshift due to the one-to-one interaction between Ca^{2+} and FA in $Ca^{2+}(FA)_1$. It should be noted that the interactions among the transition dipoles of the CO stretches are especially large, since the magnitude of the splitting for other modes of 8-O-i is as follows: $\Delta(\nu_{CN})$ = 9 cm^{-1} and $\Delta(\delta_{CH})$ = 6 cm^{-1}. The interactions among the CO oscillators, and hence the intermolecular interactions among FA molecules in the first sphere, surpass the interactions between Ca^{2+} and FA. As a result, four out of eight ν_{CO} modes of 8-O-i are

upshifted from the average value of 4RL, despite the supposed downshifts due to the $Ca^{2+}\cdots$FA interactions.

3.10. Coordination structures of Ca^{2+} in FA

Silva and Alves used the Raman spectra to determine the average number of FA molecules, N_{FA}, around Ca^{2+} [12] as already noted in section 3.7. The ν_{CO} region of the Raman spectra was decomposed into three components centered at 1680, 1705, and 1719 cm^{-1}. From the intensity of each component as a function of the salt concentration, the authors attributed the 1680 cm^{-1} component to non-coordinated FA molecules and the 1719 cm^{-1} component to FA molecules coordinated to Ca^{2+}. From a plot of the integrated intensity of the 1680 cm^{-1} component against the salt concentration, the authors derived a value of 4 for N_{FA} [12].

According to this value of N_{FA}, we first examine $Ca^{2+}(FA)_4$ complexes as a model of Ca^{2+} in FA solutions, as described in section 3.7. The theoretical IR spectra predicted for any isomers are not consistent with the experimental IR spectrum measured in this work. We suppose that the value of N_{FA} derived by Silva and Alves is not correct because of the following reason. Their assignment of the 1719 cm^{-1} component to the coordinated FA molecules is acceptable. However, we are opposed to their assignment of the 1680 cm^{-1} component solely to the non-coordinated FA molecules, because it is likely that the coordinated FA molecules also contribute to this component. As demonstrated in section 3.9, the 1667.8/1667.9 cm^{-1} modes of 8-O-i are likely to contribute to the 1680 cm^{-1} component. Much the same is true for the 1667.8 cm^{-1} mode of 7-O-i. Therefore, it is reasonable to ascribe the 1680 cm^{-1} component to both non-coordinated and coordinated FA molecules. In this case, the analysis made by Silva and Alves underestimates the value of N_{FA}.

Since a solvation number of 4 is uncommon for Ca^{2+}, Silva and Alves assumed a bidentate coordination of FA to Ca^{2+} [12]. A basic idea behind this assumption may be as follows. Bukowska studied FA solutions of Li^+ by Raman and IR spectroscopy in the ν_{CO} region [10]. When the salts were dissolved in FA, an upshifted component was newly

observed in the isotropic component of the Raman band. Meanwhile, Rode demonstrated a chelate effect by means of ab initio calculations on the $Li^+(FA)_2$ complexes [5]. He showed that a $Li^+(FA)_2$ complex with a chelate configuration, similar to 2-O-iii*, was very stable due to intermolecular NH···O hydrogen bonds and chelate energy gain. Accordingly, Bukowska adopted the 'chelate' complex as a candidate, in order to explain an anomalous intensity profile of the Raman band [10]. Later, Alves reinvestigated the same system by Raman and IR spectroscopy in wider wavenumber region [11]. Alves observed upshifts of both ν_{CN} and ν_{CO} bands and attributed the observation to a bidentate coordination of FA to Li^+. Afterward, Silva and Alves studied the Ca^{2+} system and found that the direction of the shifts of the ν_{CN} and ν_{CO} bands is the same as that of the Li^+ system [12]. In view of these results, Silva and Alves assumed a bidentate coordination of FA to Ca^{2+} with the formation of a 'chelate' ring. As demonstrated in section 3.3, however, such a 'chelate' geometry is not stable for $Ca^{2+}(FA)_2$ from DFT and MP2 calculations. Moreover, as shown in section 3.7, the ν_{CN} modes of both 'chelate' and bidentate geometries of $Ca^{2+}(FA)_4$ are downshifted; the direction is in conflict with the results of the previous and present experiments.

In addition to the 'chelate' and bidentate coordinations, the monodentate coordination via the N atom can be ruled out, because our calculations indicate that the interaction via the N atom always results in the downshifts of the ν_{CN} modes, irrespective of whether the coordination is monodentate or bidentate. Furthermore, we may discard the O-bound isomers with all FA molecules in 'trans' configuration (7-O-iii, 7-O-iv, 8-O-iii, and 8-O-iv), because the ν_{CN} modes of these isomers are downshifted from the average value of 4RL (Figs. S8 and S9 in SM). Finally, 7-O-ii and 8-O-ii may not be probable, because the strongest ν_{CO} transitions of these complexes are downshifted from that of 4RL. After all, only 7-O-i and 8-O-i remain to be candidates, which are in accord with the experimental observation that both ν_{CN} and ν_{CO} bands are upshifted. Unfortunately, it is difficult to decide between 7-O-i and 8-O-i from vibrational spectroscopic studies. We may speculate that both 7-O-i and 8-O-i are important, because the coordination structure of Ca^{2+} may be non-rigid in real solutions and FA molecules may easily come in and get out from the first solvation sphere.

In addition to vibrational spectroscopy, other experimental studies are necessary for a better understanding of the coordination chemistry of Ca^{2+} in FA.

4. Conclusions

Metal complexes of amide molecules show coordination through the O atom almost exclusively, although amides contain both O and N atoms as binding sites. So far, it has been thought that a decrease in the ν_{CO} frequency and an increase in the ν_{CN} frequency are evidence for the O atom coordination. However, upshifts of both ν_{CO} and ν_{CN} bands were observed for FA solutions of alkali and alkaline-earth metal salts. Therefore, a bidentate coordination via both O and N atoms was assumed, instead of usual monodentate coordination via the O atom.

We have shown in this work that the ν_{CN} modes of bidentate $Ca^{2+}(FA)_4$ complexes undergo downshifts, which are not consistent with the experimental observation. Instead, certain isomers of $Ca^{2+}(FA)_7$ and $Ca^{2+}(FA)_8$ complexes exhibit upshifts of both ν_{CO} and ν_{CN} modes, in spite of the monodentate coordination via the O atom. The interactions among the CO oscillators in $Ca^{2+}(FA)_7$ and $Ca^{2+}(FA)_8$ give rise to splitting of the ν_{CO} modes. The magnitude of the splitting is larger than that of the downshift supposed to occur due to the interactions between the Ca^{2+} ion and the O atom of FA. As a result, half of the ν_{CO} modes are predicted at upshifted frequencies.

It has been generally accepted that the metal–ligand interactions solely determine the direction of the frequency shifts of the intramolecular vibrations of the ligands. However, for the ν_{CO} modes of FA, the intermolecular interactions among the ligands play a dominant role in determining the direction of the shift.

Acknowledgments

The computation was carried out by using the computer facilities at Research Institute for Information Technology, Kyushu University.

Appendix A. Supplementary material

Supplementary data associated with this article can be found online at http://...

References

[1] W. Kaim, B. Schwederski, A. Klein, Bioinorganic Chemistry: Inorganic Elements in the Chemistry of Life, Wiley, New York, 2013.

[2] S.J. Lippard, J.M. Berg, Principles of Bioinorganic Chemistry, Univ. Science Books, California, 1994.

[3] P. Maslak, J.J. Sczepanski, M. Parvez, J. Am. Chem. Soc. 113 (1991) 1062–1063.

[4] D. Balasubramanian, A. Goel, C.N.R. Rao, Chem. Phys. Lett. 17 (1972) 482–485.

[5] B.M. Rode, Chem. Phys. Lett. 26 (1974) 350–353.

[6] A.J. Lees, B.P. Straugham, D.J. Gardiner, J. Mol. Struct. 54 (1979) 37–47.

[7] A.J. Lees, B.P. Straugham, D.J. Gardiner, J. Mol. Struct. 71 (1981) 61–70.

[8] D.B. Powell, A. Woollins, Spectrochim. Acta A 41 (1985) 1023–1033.

[9] J. Bukowska, K. Miaskiewicz, J. Mol. Struct. 74 (1981) 1–10.

[10] J. Bukowska, J. Mol. Struct. 98 (1983) 1–10.

[11] W.A. Alves, J. Mol. Struct. 829 (2007) 37–43.

[12] E.F. Silva, W.A. Alves, Vib. Spectrosc. 62 (2012) 264–267.

[13] T.B.C. Campos, E.F. Silva, W.A. Alves, Vib. Spectrosc. 65 (2013) 24–27.

[14] M.J. Frisch, G.W. Trucks, H.B. Schlegel et al., GAUSSIAN 16, Revision A.03, Gaussian Inc., Wallingford CT, 2016.

[15] E.C. Lee, H.M. Lee, P. Tarakeshwar, K.S. Kim, J. Chem. Phys. 119 (2003) 7725–7736.

[16] D. McNaughton, C.J. Evans, S. Lane, C.J. Nielsen, J. Mol. Spectrosc. 193 (1999) 104–117.

[17] I. Suzuki, Bull. Chem. Soc. Jpn. 41 (1960) 1359–1365.

[18] I. Bakó, T. Megyes, S. Bálint, V. Chihaia, M.-C. Bellissent-Funel, H. Krienke, A. Kopf, S.-H. Suh, J. Chem. Phys. 132 (2010) 014506.

[19] A. Pullman, H. Berthod, C. Giessner-Prettre, J.F. Hinton, D. Harpool, J. Am. Chem. Soc.

100 (1978) 3991–3994.

[20] M. Asada, T. Fujimori, K. Fujii, R. Kanzaki, Y. Umebayashi, S. Ishiguro, J. Raman Spectrosc. 38 (2007) 417–426.

[21] H. Torii, M. Tasumi, J. Phys. Chem. B 102 (1998) 315–321.

Figure Captions

Fig. 1. ATR-IR spectra in the 1200–1800 cm^{-1} region: (a) neat FA liquid, (b) 1.0 M, (c) 2.0 M, (d) 3.0 M, and (e) 4.0 M solutions of $Ca(ClO_4)_2$ in FA at ambient temperature. Amplitude of all spectra is normalized to have the same maximum height. Dashed lines indicate the positions of band maxima in the spectrum of neat FA liquid.

Fig. 2. Optimized structures and theoretical IR spectra of (a) FA monomer and $Ca^{2+}(FA)_1$ complexes: (b) 1-O-i, (c) 1-O-ii, (d) 1-N, and (b) 1-ON. Interactions between Ca^{2+} and FA are indicated by dashed lines. Amplitude of the spectra of 1-N and 1-ON is magnified by a factor of 1.5 and 2, respectively. The 1241 cm^{-1} transition of 1-ON is due to NH_2 wag and the 1685 cm^{-1} transition partly bears a character of CO stretch.

Fig. 3. Structures and theoretical IR spectra of (a) FA monomer and $Ca^{2+}(FA)_2$ complexes: (b) 2-O-i, (c) 2-O-ii, (d) 2-ON*, and (e) 2-O-iii*. Both 2-ON* and 2-O-iii* (with an asterisk symbol) are not stationary but instantaneous geometries during optimization processes. Amplitude of the spectrum of 2-ON* is magnified by a factor of 2.

Fig. 4. Geometries of $Ca^{2+}(FA)_4$ complexes: (a) 4-O-vii*, (b) 4-O-viii*, (c) 4-ON-i*, (d) 4-ON-ii*, (e) 4-N*, and (f) 4-O-i. The $Ca^{2+}\cdots O/Ca^{2+}\cdots N$ distances are in the ranges of 2.32–2.33/3.08–3.12 Å in 4-O-vii*, 2.32/3.00–3.04 Å in 4-O-viii*, 2.65–2.79/2.92–2.99 Å in 4-ON-i*, and 2.60–2.64/2.81–2.83 Å in 4-ON-ii*. The $Ca^{2+}\cdots N$ distances are in the ranges

of 2.82–2.84 Å in 4-N*. The $Ca^{2+}\cdots O$ distances are 2.37 Å in 4-O-i.

Fig. 5. Theoretical IR spectra of (a) structure 4RL of $(FA)_4$ and $Ca^{2+}(FA)_4$ complexes: (b) 4-O-vii*, (c) 4-O-viii*, (d) 4-ON-i*, (e) 4-ON-ii*, (f) 4-N*, and (g) 4-O-i. Dashed curve in (a) stands for experimental IR spectrum of neat FA liquid. Amplitude of the spectra in the 1200–1500 cm^{-1} region is magnified by a factor of 3. Amplitude of the spectra of 4-ON-i*, 4-ON-ii*, and 4-N* is magnified by a factor of 2, 1.5, and 2, respectively.

Fig. 6. Optimized structures of lowest-energy isomers of $Ca^{2+}(FA)_n$ complexes with n = 5–8: (a) 5-O-i, (b) 6-O-i, (c) 7-O-i, and (d) 8-O-i. These structures are also displayed in Figs. S6–S9 of SM.

Fig. 7. Theoretical IR spectra for (a) 4RL of $(FA)_4$ and lowest-energy isomers of $Ca^{2+}(FA)_n$ complexes with n = 4–8: (b) 4-O-i, (c) 5-O-i, (d) 6-O-i, (e) 7-O-i, and (f) 8-O-i. Amplitude of the spectra in the 1200–1500 cm^{-1} region is magnified by a factor of 3. Dashed curve in (a) stands for experimental IR spectrum of neat FA liquid. Location of the strongest ν_{CO} transition(s) is as follows: 1671.9 cm^{-1} (4RL), 1670.4/1671.3 cm^{-1} (4-O-i), 1670.0/1671.4 cm^{-1} (5-O-i), 1669.6 cm^{-1} (6-O-i), 1675.5/1676.0/1677.0 cm^{-1} (7-O-i), and 1683.3 cm^{-1} (8-O-i).

Fig. 8. Comparison of experimental (a) IR and (d) Raman spectra of 4.0 M solution with theoretical (b) IR and (c) Raman spectra predicted for 8-O-i. Experimental Raman spectrum is taken from the literature [12].

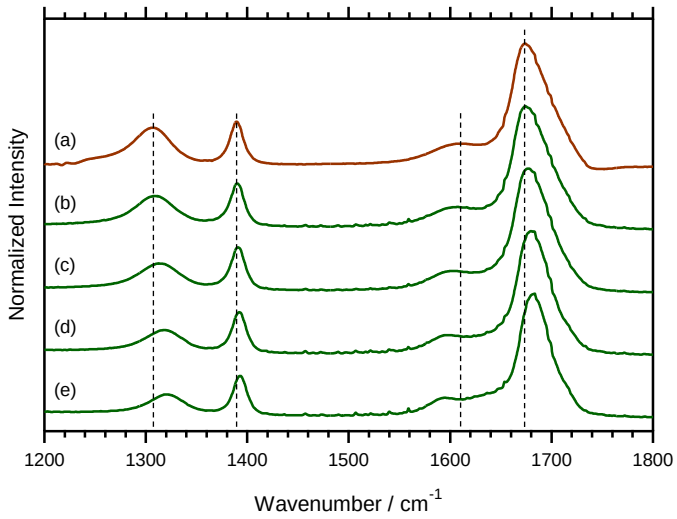

Fig. 1. Ohashi et al.

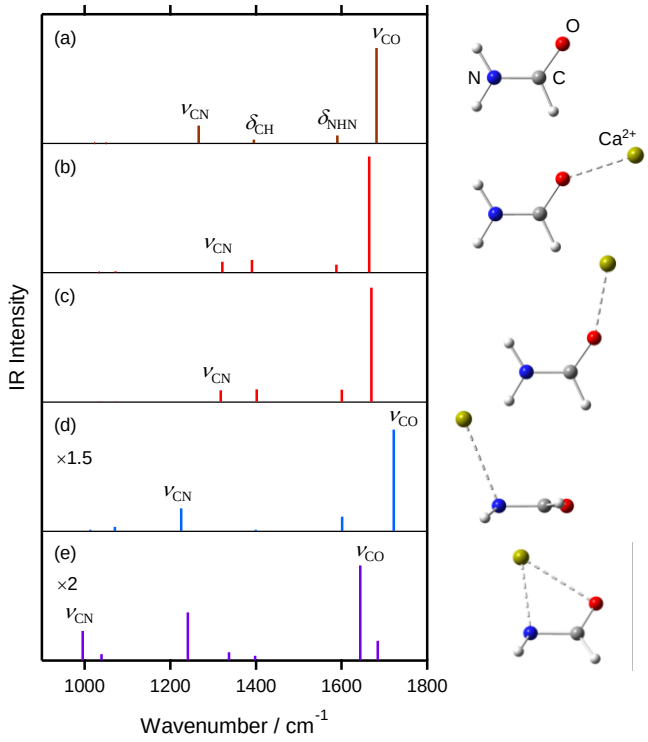

Fig. 2. Ohashi et al.

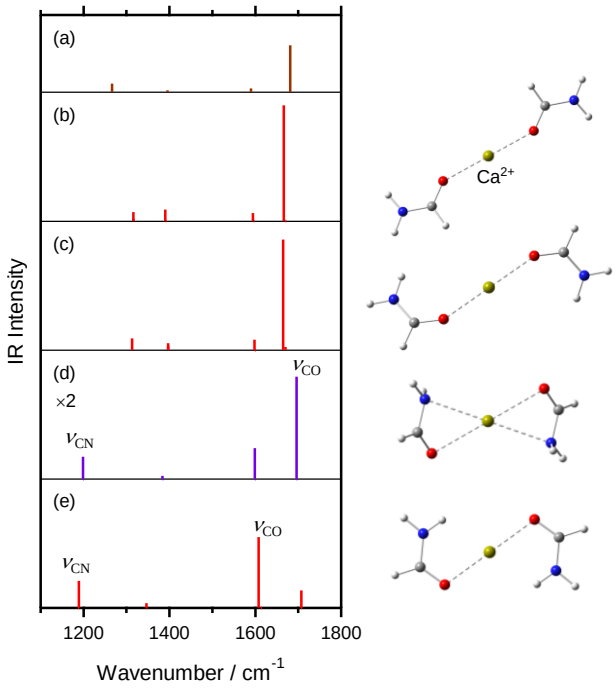

Fig. 3. Ohashi et al.

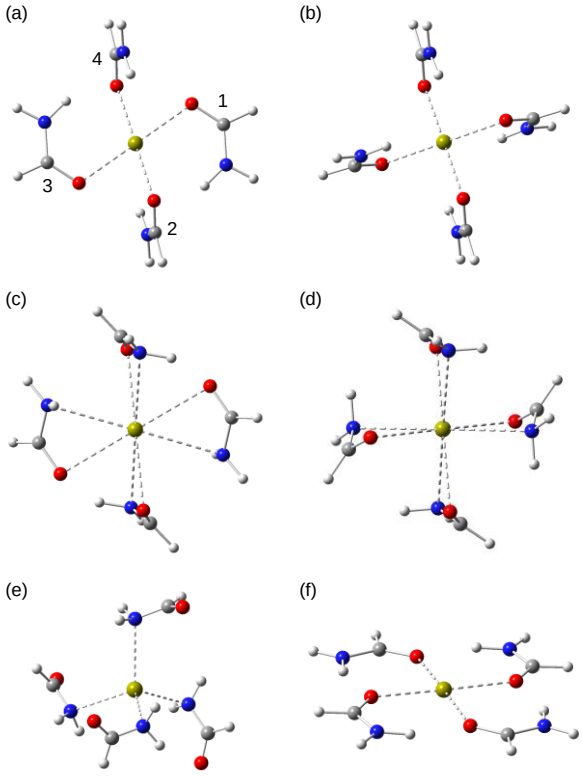

Fig. 4. Ohashi et al.

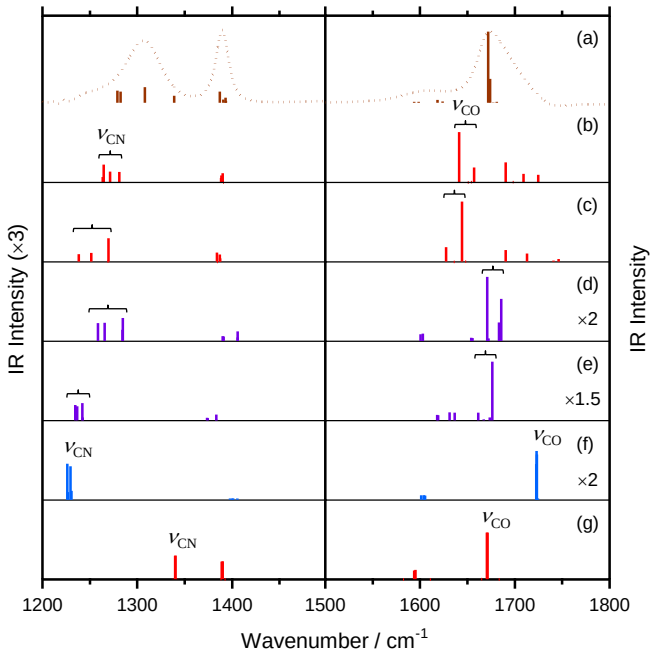

Fig. 5. Ohashi et al.

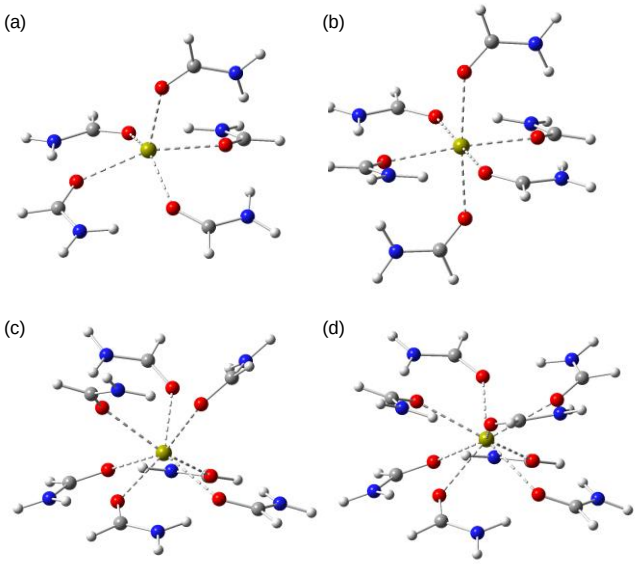

Fig. 6. Ohashi et al.

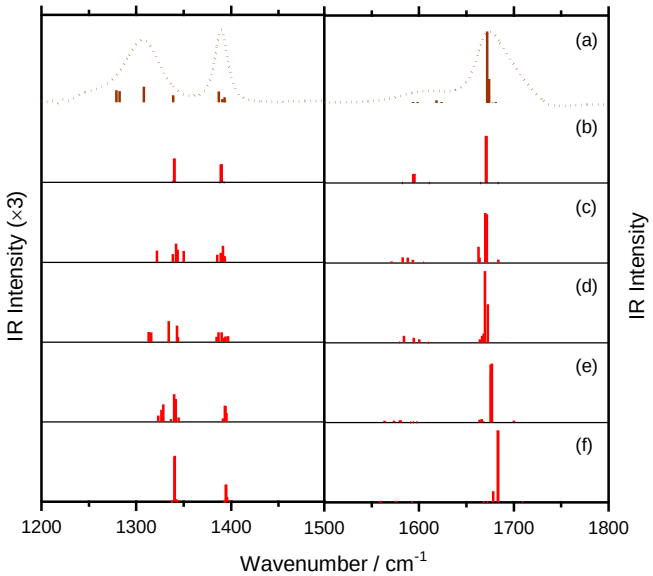

Fig. 7. Ohashi et al.

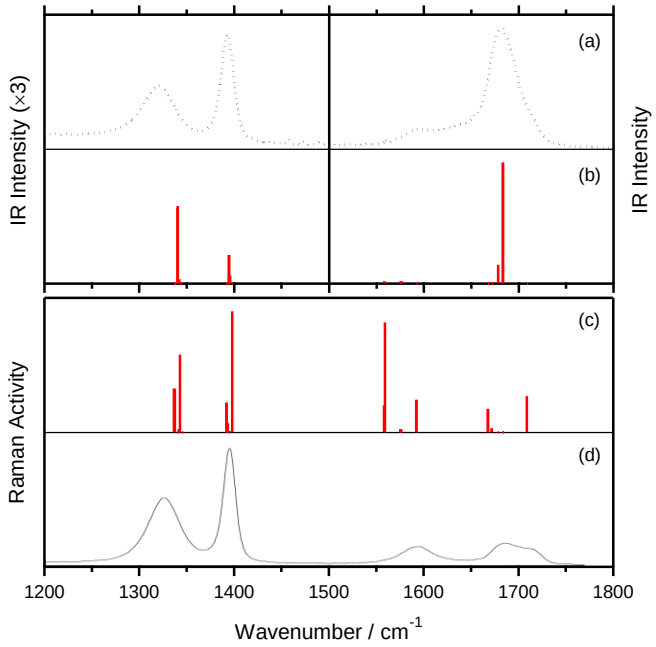

Fig. 8. Ohashi et al.